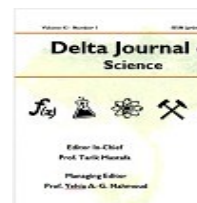




Delta Journal of Science

Available online at <https://djs.journals.ekb.eg/>

Research Article

CHEMISTRY

Photophysical Behavior and Sensing Response of Chalcone Containing Pyrene moiety

Marwa N. El-Nahass, Tarek A. Fayed*, Saleh Abd Elazim, Doaa F. Draz, Fathy Hassan

Department of Chemistry, Faculty of Science, Tanta University, Tanta, Egypt

* Corresponding Author: Dr. Tarek A. Fayed

E-mail: tfayed2013@gmail.com

KEY WORDS

Dyes,
solvatochromism,
optical materials,
surfactants,
sensors

ABSTRACT

D- π -A dye composed of pyrene and thiophene units was synthesized and characterized using elemental, FT-IR, and mass analyses. The solvatochromic response was investigated in different solvents of various polarities. Additionally, the inclusion characteristic of the investigated dye was studied in different organized assemblies of three surfactants. The spectral changes suggested that the dye would be useful to study the critical micelle concentrations of the studied assemblies systems. Furthermore, the absorption and emission spectra are sensitive towards H⁺, Co²⁺, Ni²⁺, Cd²⁺, Pb²⁺, and Zn²⁺ ions owing to acido- and metallochromic behaviors. These results suggest that the investigated dye would be potential candidate for polarity sensors, probe to characterize microenvironmental polarity of the surfactants, and sensor for metal ions and H⁺ proton.

1. Introduction

Solvatochromic and charge transfer behaviors of D- π -A dyes have received a considerable attention owing to a growing

interest in different fields [1, 2]. These dyes have used for determination of the solvent polarity [3], as colorimetric

chemosensors for volatile organic compounds [4,5], photo- and electroluminescent materials in dye lasers [6,7], switchable viscosity probes [8], dual-ion-switched molecular brakes [9], dye sensitized solar cells [10–12] and nonlinear optical materials [13]. Among of these dyes, chalcones are great of interest chemo types for both chemists and physicists, due to their high natural abundance, easy synthesis, and their diverse biological activities. Additionally, they have been used as photorefractive polymers, holographic recording materials, and fluorescent probes for different metal ions sensing [14–20]. On the other hand, the polycyclic aromatic hydrocarbons such as naphthalene, phenanthrene, and pyrene have strong absorption cross section, excellent emission properties, and long excited state lifetime compared to simple phenyl analogue [21, 22].

In this study, we designed new D- π -A dye composed of polycyclic aromatic hydrocarbon (pyrene) and thiophene as chromophores units. The import of those aromatic units as terminal groups will influence the polarity and viscosity environment of the fluorescence characteristics of the dye. Further, introducing polycyclic aromatic ring will influences the noncentrosymmetric crystal packing of dye owing to π - π

stacking interaction. In addition, the molecular hyperpolarizability is strongly influenced not only by the electronic effect but also by the steric effect of the substituent.

The molecular design of the synthesized dye is shown in Fig. 1. The dye was abbreviated as follow: 3-(4,5-dihydropyren-2-yl)-1-(thiophen-2-yl) prop-2 en-1-one (**PyTPO**). The solvent effect on the investigated dye was discussed. The spectral behavior in organized assemblies of micelles (SDS, CTAB and, TX-100) was also studied to evaluate the ICT emission and inclusion behaviors to explore its probing ability to characterize the properties of these media. Further, the sensing response towards different metal ions such as Co^{2+} , Ni^{2+} , Cd^{2+} , Pb^{2+} , and Zn^{2+} was investigated. In addition, the acidochromic behavior of the investigated dye was studied using Hammett's acidity function scale (H_0).

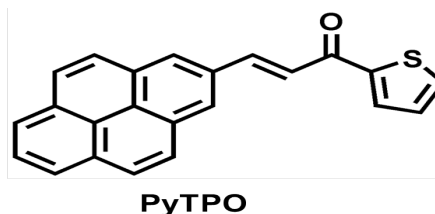


Fig.1. Chemicals structures of the investigated dye.

2. Experimental

2.1. Materials

All chemicals were purchased from Merck-Aldrich Chemicals and used as received without further purification: 2-acetyl thiophene, 9-pyrene carbaldehyde, sodium dodecyl sulfate (SDS), cetyltrimethyl ammonium bromide (CTAB), Triton X-100 (TX-100), metal salts ($\text{CoCl}_2 \cdot 6\text{H}_2\text{O}$, $\text{NiCl}_2 \cdot 6\text{H}_2\text{O}$, CdCl_2 , PbCl_2 , and ZnCl_2), and solvents (methanol (MeOH), acetonitrile (ACN), dichloromethane (CH_2Cl_2), benzene (Benz) and n-heptane (Hep). All solvents were found to be non-fluorescent in the scanned range.

2. 2. Methods

The FT-IR spectra were recorded by JASCO FT/IR-4100 spectrophotometer using KBr Pellets within the range 4000 to 400 cm^{-1} . Mass spectrum was measured on a Finnigan MAT 8222 EX mass spectrometer at 70 eV. The elemental microanalyses of the investigated dye were performed using Perkin-Elmer 240 CHNS Elemental analyzer. Steady-state absorption and emission spectral measurements were carried out using a Shimadzu UV-3101PC scanning spectrophotometer and Agilent Cary Eclipse Fluorescence Spectrophotometer, respectively. In all experiments, 2×10^{-5} M solutions were used and handled under dim light at room temperature. The fluorescence quantum

yield (Φ_f) of the investigated dye was measured using the optically diluted solution to avoid the reabsorption effect (absorbance at excitation wavelength ≤ 0.1), relative to the method with a solution of quinine sulfate in 0.5 mol/dm^3 H_2SO_4 ($\Phi = 0.55$) [23].

2.3. Synthesis

The investigated dye was synthesized following the protocol of previous report [24]. The molecular structure was confirmed by FT-IR, mass spectroscopy, and elemental analysis. The FT-IR spectrum showed sharp bands at vibrational frequencies within the range 1587 cm^{-1} and 1643 cm^{-1} characteristic for the ethylenic double bond and carbonyl group, respectively, Fig. 2. The spectra showed bands at 917 - 1085 cm^{-1} owing to out of plane bending vibration of $\text{CH}=\text{CH}$. In addition, weak bands are observed in the range 3423 - 3448 cm^{-1} corresponding to stretching vibrations of the aliphatic C-H bond. The mass spectrum of the investigated dye shows molecular ion peaks at the desired positions: $m/z = 338$, Fig.3. The obtained molecular ion peaks showed that m/z is equivalent to the molecular weight of the proposed compounds. Hence, m/z value confirms the molecular weight of the investigated dye. Elemental analysis: calcd for $\text{C}_{23}\text{H}_{14}\text{SO}$; C, 81.65; H, 4.14 and S, 9.47;

Found: C, 85.52; H, 4.17 and S, 9.76, mp 170 °C.

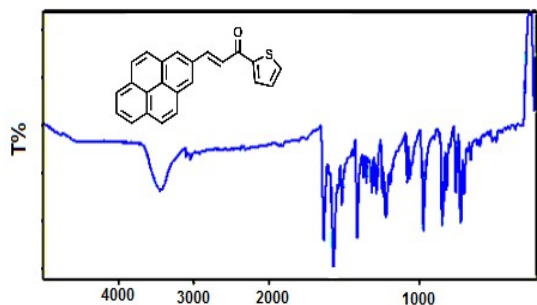


Fig. 2: FT-IR spectrum of the investigated dye.

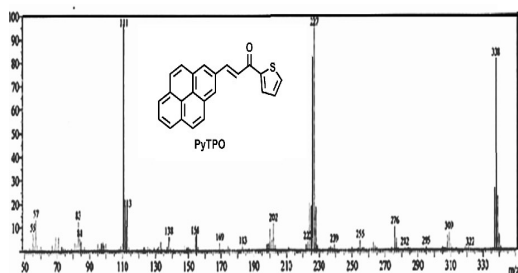


Fig.3: Mass spectrum of the investigated dye.

3. Results and Discussion

a. Solvatochromic behavior of the investigated dye

Steady state absorption and fluorescence spectra of the investigated dye have been studied in solvents of different polarities at room temperature, [Fig. 4 \(a\)](#), and the corresponding spectroscopic data were summarized in [Table 1](#). As can be seen, the absorption spectra of **PyTPO** showed vibrational structure in all used solvents owing to the planar structure of the pyrene moiety of as shown in [Fig.5](#). In addition, the absorption band of the investigated dye undergoes red shifts with changing the solvent polarities. This absorption band may be due to the

intramolecular charge transfer from the aryl moiety (pyrene) to the carbonyl group via the ethylenic bridge (push-pull dye π -system).

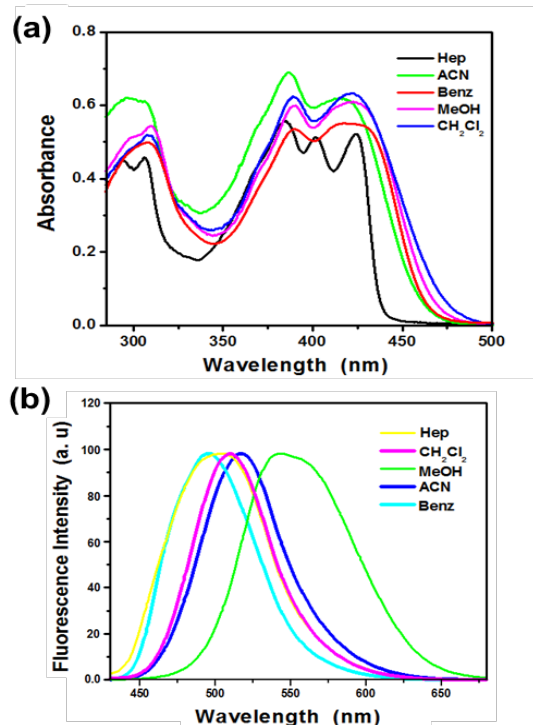


Fig. 4: Absorption (a) and emission (b) spectra in different polarities solvents of **PyTPO**.

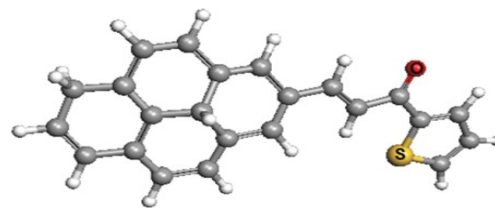


Fig.5: Optimized structures of the investigated dye.

As shown in [Table 1](#), the absorption spectrum of the dye under investigation is less sensitive to the solvent polarity compared to the fluorescence spectra, indicating that the excited singlet states of **PyTPO** molecule have more polar character than its ground state. Further,

emission spectra of the investigated dye are represented in Fig. 4 (b). The fluorescence spectrum suffers a strongly bathochromic shift as the solvent polarity is increased by 44 nm, from MeOH to Hep, for **PyTPO**, indicating the ICT from the aryl moiety to the carbonyl group which takes place within the molecule in the singlet excited state S_1 . This suggests that the molecule are solvated significantly in the S_1 excited state, resulting in a bathochromic shift and observable difference in the dipole moment between the S_1 excited state and the ground state S_0 .

As the emission spectra of the investigated dye are strongly affected by the solvent in aspects of emission intensity and wavelength, the visual effect of the polarity dependence of the fluorescence of **PyTPO** was examined. **PyTPO** dye gave an interesting feature via the irradiation at $\lambda_{ex}=365$ nm in all used solvents. It can be seen clearly that with increasing the solvent polarity, the fluorescence of **PyTPO** is greatly intensive in protic and aprotic solvents and quenched significantly in non-polar solvent such as Hep and Benz, therefore **PyTPO** can be used as polarity probes.

A cursory glance on the data reported in Table 1, it was found that the fluorescence quantum yields (Φ_f) are

highly sensitive to the solvent polarity and the ring size. The Φ_f values of **PyTPO** increase by 1.98 folds on going from Hep to MeOH. The results indicate that **PyTPO** is highly fluorescent dye.

Table 1: Dipole moments and correlation factor (R) of **PyTPO** measured in various solvents at 25 °C.

Solvent	λ_{max}^a (nm)	λ_{max}^f (nm)	Φ_f	μ_g (D)	μ_e (D)
Hep	385,424	501	0.05	1.6	21.9
Benz	390,421	495	0.34		
CH ₂ Cl ₂	389,421	510	0.55		
ACN	387,417	517	0.56		
MeOH	389,423	545	0.099		

Also, the difference in the dipole moments between the excited singlet (μ_e) and ground (μ_g) states can be determined using Bakhshiev's and Kawski-Chamma-Viallet's [25]. The Onsager cavity radius, a , was estimated following geometry optimization of the investigated dye (with the help of ArgusLab 4.0 software and free HyperChem 8.03 software using PM3 Hamiltonian method) and comes out to be 6.4 Å.

The dipole moments of the investigated dye in both ground and excited states have been estimated. As can be seen, the dipole moment of the investigated dye in the ground state was smaller than that reported in the excited state, confirming the existence of a more

relaxed excited state, due to ICT favored by the cooperative effects of the aryl moiety as a donor and the carbonyl fragment as an acceptor. The large difference between the dipole moments of ground and excited states is consistent with the higher extent of contribution of dipole-dipole interaction towards the stability of excited state than that of ground state. This result suggests that this dye can serve as good candidate components of nonlinear optical materials.

3.2. Effect of surfactant on the spectral behavior of the investigated dye

The spectral properties of the investigated dye have been studied in cationic, CTAB, anionic, SDS, and neutral, TX-100, micellar media. Fig. 6 shows the absorption spectra of the investigated dye in the absence and presence of different concentrations of the used surfactant. Generally, it was found that the absorption spectra for **PyTPO** increase with increasing the concentrations of the used surfactants with hypsochromic shift. The absorption bands in water (located at 440 nm) are blue shifted by 5 nm, 13 nm, and 16 nm on adding different concentrations of CTAB, SDS, and TX-100, respectively.

The fluorescence band maximum of **PyTPO** located at 539 nm in water is strongly blue shifted ca. 32, 16 and 38 nm

on adding CTAB, SDS, and TX-100, respectively, which are very close to the critical micelle concentration (CMC). The spectral shift is accompanied by a great enhancement in the fluorescence intensity, confirming the stronger binding between the used surfactants and **PyTPO** dye. The continuous enhancement in the fluorescence intensity is attributed to the passage of dye molecule from the aqueous bulk solution to the palisade layer of the micelle. The decrease in polarity of the microenvironment around the dye molecule results in the reduction of the non-radiative transfer rate from the ICT state to the low-lying singlet or triplet state due to the increase in the energy gap between them, which leads to an increase in emission intensity. In CTAB and SDS, the dipolar excited **PyTPO** molecules will be transferred to a less-polar hydrophobic environment, and their head groups try to increase the fluorescence intensity by pushing the dye molecule towards nonaqueous environment. However, in the case of TX-100, the driving force is hydrophobic, which makes the dye molecule more compact, more rigid and less mobile.

The situation is some extent different on recording the fluorescence spectra of **PyTPO** in the presence of CTAB and SDS. Moreover, more significant reductions were noticed in the

fluorescence intensities. It seems that the dye molecules located at the micelle-water interface, showing the quenching role of water.

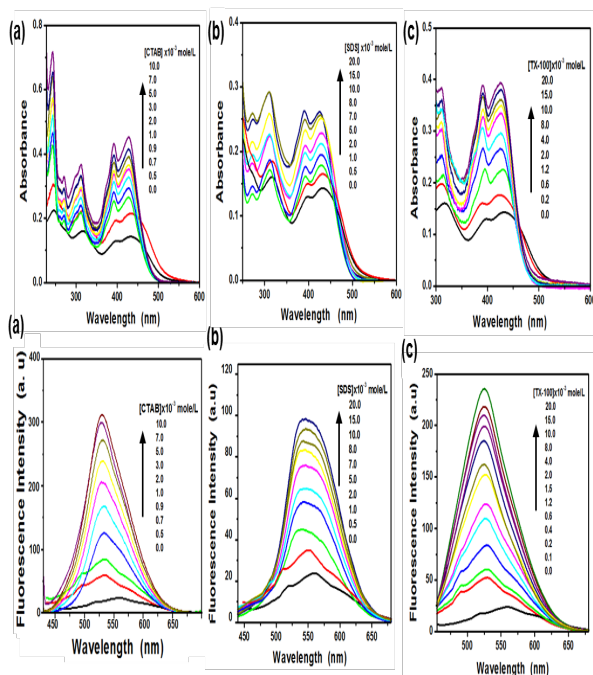


Fig.6: Absorption and fluorescence spectra of **PyTPO** measured in CTAB (a), SDS (b), and TX-100 (c) micellar solutions, respectively.

investigated dye

In order to study the effect of acidity on the spectral behavior of **PyTPO**, the electronic absorption and emission spectra of 2×10^{-5} mol/L of the investigated dye were measured at different concentrations of sulfuric acid, **Fig.7**. The absorption spectra of the investigated dye changed dramatically upon increasing the concentration of sulfuric acid (from 10% to 98%) with an observable change in color, **Fig.8**. As a

representative example, **PyTPO** dye solution changes from faint yellow, to violet passing through faint blue color as the concentration of sulfuric acid was increased. Actually, the yellow color is recovered upon the addition of water solution, which is evidence for the reversibility of the prototropic equilibrium that takes place.

On the other hand, the fluorescence maximum of the neutral species which appears at $\lambda_{\max}^f = 562$ nm, is red-shifted by 21 nm, at lower sulfuric acid concentrations (from 10%-40%), however, at high concentrations (from 50% to 70%), the fluorescence maximum is blue-shifted ($\lambda_{\max}^f = 485$ nm). Two bands have been developed at 476 and 645 nm, respectively, at very high concentrations 90% and 98%.

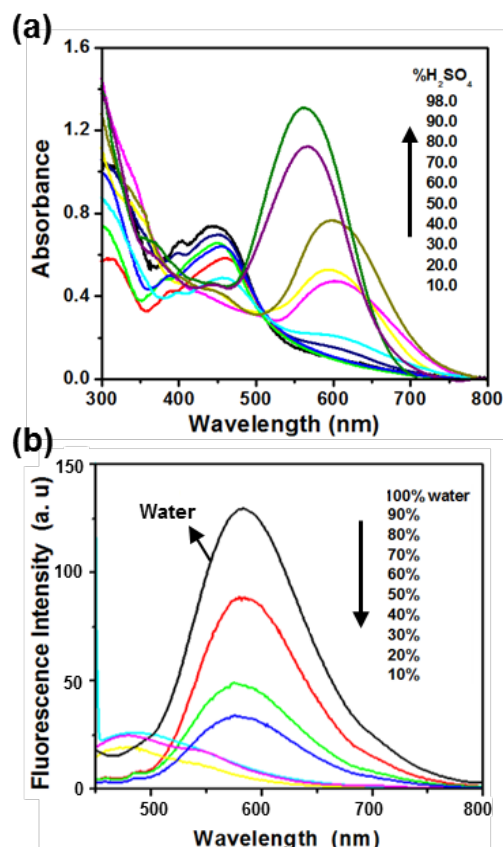


Fig.7: Absorption (a) and emission (b) spectra for **PyTPO** upon addition of different concentrations of sulfuric acid.

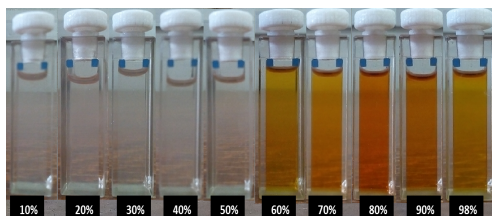


Fig. 8: Acidochromic behavior of **PyTPO** in sulfuric acid solutions.

3.3. Metallochromic behaviors of the investigated dye

The sensing ability of the investigated dye, towards the metal ions such as Co^{2+} , Ni^{2+} , Cd^{2+} , Pb^{2+} , and Zn^{2+} has been studied. Figure 9 shows the electronic absorption spectra of **PyTPO** in the absence and presence of different

concentrations of the used metal ions in ethanolic solution. As shown, on adding Co^{2+} ions to 2×10^{-5} M dye solution, the absorption band maximum appearing at 425 nm decreases with appearance of a new visible absorption band at 656 nm. This was accompanied by formation of isosbestic point at 466 nm. Also, for the interaction of **PyTPO** with Ni^{2+} , the absorption band maxima increase with formation of isosbestic point at 390 nm. However, in case of adding different concentrations of Pb^{2+} to **PyTPO** solutions, the absorption band increases gradually with formation of a broad band at 489 nm. The similar behavior for Zn^{2+} ion, at which a broad band at 500 nm, has been observed. The obtained results could be explained on the basis of complex formation between the used metal ions and the investigated **PyTPO** through sulfur atom of thiophene moiety and the oxygen atom of the carbonyl group. This suggests that the investigated dye exhibit high sensitivity towards the used metal ions.

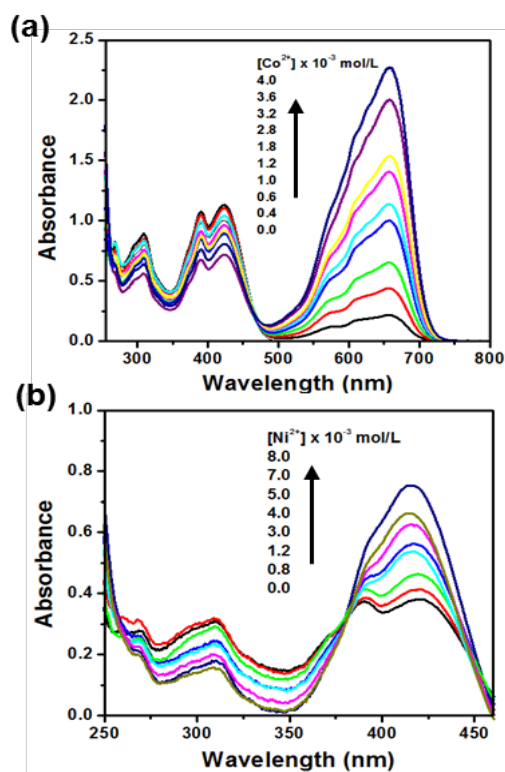


Fig. 9: The absorption spectra of PyTPO after addition of (a) $[\text{Co}^{2+}]$ and (b) $[\text{Ni}^{2+}]$ ions.

Figure 10 shows the emission spectra of PyTPO in the presence of different concentrations of the mentioned metal ions. The fluorescence band of the investigated dye observed at 553 nm in EtOH, was hypochromic shift on adding different concentrations of Co^{2+} , Ni^{2+} , and Zn^{2+} ions by (6, 14, 3 nm), (9, 5, 3 nm), and (5, 8, 6 nm), respectively, with a great quenching in the fluorescence intensity. Upon adding different concentrations of both Pb^{2+} , and Cd^{2+} ions, the fluorescence spectra increase with bathochromic shift. The results confirm the complexation between the

investigated dye and the mentioned metal ions.

The ground and excited state binding constants of Co^{2+} , Ni^{2+} , Cd^{2+} , Pb^{2+} , and Zn^{2+} complexes with the investigated dye were determined by employing Benesi Hildebrand equation [26]. The obtained data indicates that Cd^{2+} is the strongest binding metal ions with the investigated chemosensor than the other tested metal ions, indicating that Cd^{2+} is the most effectively detected and the potential of the novel dye as highly efficient switchers for Cd^{2+} ions.

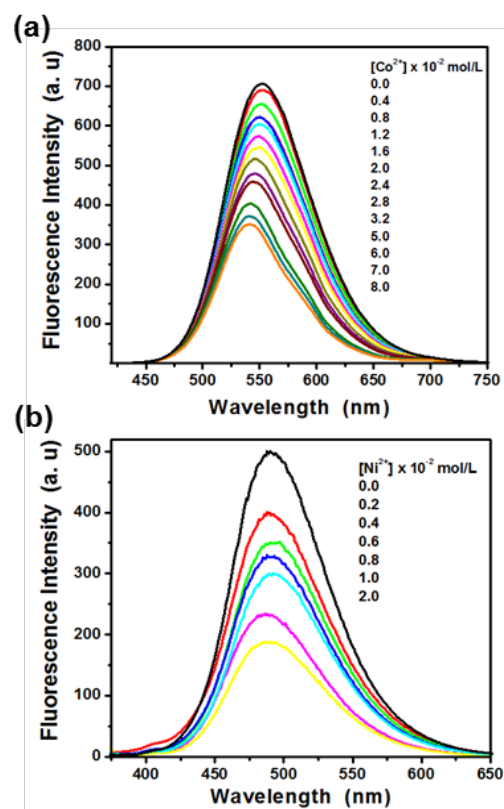


Fig.10: Emission spectra of PyTPO after addition of (a) $[\text{Co}^{2+}]$ and (b) $[\text{Ni}^{2+}]$ ions.

4. Conclusion

Pyrene-thiophene dyes was successfully synthesized and characterized. Large excited state dipole moments were obtained from the fluorescence spectra, indicating the stabilization of the excited state in polar solvents owing to solvatochromic behavior. In addition, a change in the dye color in various solvents was observed, suggesting its potential as candidate probes for the identification of organic solvents. The investigated dye was used also to study the microenvironmental polarity and evaluation of critical micelle concentrations of three different surfactants. Furthermore, acido- and metallo-chromic behaviors were observed from absorption and emission spectra with color change with efficient reversibility. These results suggest that the investigated dye would be potential candidate for polarity sensors, probes to characterize microenvironmental polarity and critical micelle concentrations of surfactants, and sensors for metal ions and H⁺ proton.

5. References

1. A. Klymchenko, *Acc. Chem. Res.*, 2017, **50**,366.
2. B. Carlotti, A. Cesaretti, O. Cannelli, T. Giovannini, C. hiaraCappelli, C. Bonaccorso, C. Fortuna, F. Elisei, A. Spalletti, *J. Phys. Chem. C*, 2018, **122**, 2285.
3. E. Verbitskiy, E. Cheprakova, J. Subbotina, A. Schepochkin, P. Slepukhin, G. Rusinov, V. Charushin, O. Chupakhin, N. Makarova, A. Metelitsa, V. Minkin, *Dye Pigments*, 2014, **100** , 201.
4. Bamfield P. (2001) Chromic phenomena: technological application of colour chemistry. The Royal Society of Chemistry, Cambridge.
5. M. Janzen, J. Ponder, D. Bailey, C. Ingison, K. Suslick, *Anal. Chem.* 2006, **78**, 3591.
6. V. Anthonov, K. Hohla, *Appl. Phys. B*, 1983, **32**, 9.
7. S. Speiser, N. Shakkour, *Appl. Phys. B* 1985, **38**, 191.
8. A. Silva, H. Gunaratne, T. Gunnlaugsson, A. Huxley, C. McCoy, J. Rademacher, T. Rice, *Chem. Rev.* 1997, **97**,1515.
9. D. Zhang, Q. Zhang, J. Su, H. Tian, *Chem. Commun.* 2009, 1700.
10. J. Sansregret, J. Drake, W. Thomas, M. Lesiecki, *Appl Opt* 1983, **22**, 573.
11. B. Liu, W. Zhu, Q. Zhang, W. Wu, M. Xu, Z. Ning, Y. Xie, H. Tian, *Chem. Commun.* 2009, 1766.
12. E. Verbitskiy, E. Cheprakova, J. Subbotina, A. Schepochkin, P. Slepukhin, G. Rusinov, V. Charushin, O. Chupakhin, N. Makarova, A. Metelitsa, V. Minkin, *Dye Pigments*, 2014, **100**, 201.

13. X. Zhang, B. Chen, X. Lin, Q. Wong, C. Lee, H. Kwong, S. Lee, S. Wu, *Chem. Mater.*, 2001, **13**, 1565.
14. Y. Wei, G. Qin, W. Wang, W. Biana, S. Shuang, C. Dong, *J. Lumin.*, 2011, **131**, 1672.
15. G. Gillispie, *Adv. Chem.*, 1993, **236**, 89.
16. M. N. El-Nahass, D. M. Abd El-Aziz, T. A. Fayed, *Sens. Actuat B-Chem.*, 2014, **205**, 377.
17. M. El-Nahass, T. Fayed, *Appl. Organomet. Chem.*, 2017, **31**, 1.
18. Marwa N. El-Nahass, Tarek A. Fayed, Mohamed H. Shaaban, Fathy M. Hassan, *Sens. Actuat. B Chem.*, 2015, **210**, 56.
19. Faten M. Atlam, Marwa N. El-Nahass, Eman A. Bakr, Tarek A. Fayed, *Appl. Organomet. Chem.*, 2017.
20. M. Gaber, Tarek A. Fayed, Marwa N. El-Nahass, H.A. Diab, Mohammed M. El-Gamil, *Appl Organometal Chem.*, 2019, **33**, e5133
21. R. Liu, H. Ran, Z. Zhao, X. Yang, J. Zhang, L. Chen, H. Sun, and J. Hu, *ACS Omega*, 2018, **3**, 5866.
22. E. Gutiérrez, M. Percino, V. Chapela, M. Cerón, J. Maldonado, G. Ortiz, *Materials*, 2011, **4**, 562.
23. J. Demas, G. Crosby, *J. Phy. Chem.*, 1971, **75**, 991.
24. T. Fayed, M. El-morsi, M. El-Nahass, *J. Photochem. Photobio. A*, 2011, **224**, 38.
25. a) N. Bakshiev, *Opt. Spectosc.*, 1964, **16**, 821; b) A. Kawski, *Acta Phys. Pol.*, 1966, **29**, 507; c) A. Chamma and P. Viallet, *C. R. Seances Acad. Sci., Ser. C*, 1970, **27**, 1901.
26. M. Benesi, J. Hildebrand, *J. Am. Chem. Soc.* 1949, **71**, 2703

الخصائص الضوئية الفيزيائية والاستجابة المجسية لمركب الشالكون المحتوى على حلقتي بيرين وثنيوفين

إد/ طارق عبد المنعم فايد، إد/ صالح عبد العظيم عطيه، إد/ مروه نبيه النحاس، د. فتحى مدحت حسن، دعاء فوزى دراز

قسم الكيمياء- كلية العلوم- جامعة طنطا

تم تحضير وتوصيف مستشعر فلوريسيني للشالكون. وتم فحص الاستجابة في المذيبات ذات القطبية المختلفة. تم دراسة الصفات الضوئية في أوساط مختلفة من (CTAB)، (SDS)، (TX-100)X-100. التغيرات في القياسات الطيفية أشارت الي ان الاصباع تحت الدراسة ستكون مفيدة لدراسة البنية الدقيقة وتقدير التركيزات الحرجة لانظمة المجموعات المدروسة. علاوة على ذلك، فإن أطيف الامتصاص والانبعاث أظهرت حساسية تجاه أيون الهيدروجين H^+ ، وايونات المعادن (Co^{+2} ، Ni^{+2} ، Cd^{+2} ، Pb^{+2} ، Zn^{+2}). هذه النتائج تشير إلى أن الأصباع التي تم فحصها ستكون مرشحاً محتملاً لأجهزة استشعار القطبية، ومناسبة لتوصيف قطبية البنية الدقيقة والتركيزات الحرجة للميسل، وايضا أجهزة استشعار أيونات المعادن وأيون الهيدروجين H^+ .